

# Fourier transform Raman spectra of tin(IV) tetraphenylporphyrin complexes

Dennis P. Arnold

School of Chemistry, Queensland University of Technology, G.P.O. Box 2434, Brisbane 4001 (Australia)

(Received October 28, 1991)

## Abstract

Solid state non-resonance Raman spectra of a series of tin(IV) *meso*-tetraphenylporphyrin complexes  $\text{Sn}(\text{TPP})\text{X}_2$ , and the free ligand  $\text{H}_2\text{TPP}$ , have been collected using 1064 nm laser excited Fourier transform Raman spectroscopy. The application of this technique to strongly coloured and fluorescent compounds is thereby demonstrated. The axial ligands  $\text{X}^-$  include a set of eight O-bound anions of widely differing basicity, and the four halides. The relationships between Raman band frequencies and the nature of the axial ligands are examined. The data are compared with previously published empirical correlations between Raman frequencies and geometrical parameters.

## Introduction

Porphyrins and their metal complexes have been the subjects of extensive study by resonance Raman (RR) spectroscopy [1, 2]. Porphyrins absorb light strongly throughout the visible and near-UV regions and the free ligands and many complexes also exhibit fluorescence and phosphorescence. This has encouraged the use of the resonance technique and almost completely precluded the use of conventional Raman excitation. The recent availability of Fourier transform Raman instruments with excitation by the near-IR Nd/YAG laser (1064 nm) opens the door to increased use of conventional Raman spectra for such species as metalloporphyrins. The inherent weakness of Raman scattering can be overcome by long spectral accumulation and subsequent Fourier transformation. This allows the use of very low laser power, thus avoiding decomposition, and the 1064 nm excitation should, in principle, avoid problems of self-absorption and fluorescence background.

RR spectroscopy of porphyrins has been an important tool in probing many aspects of their chemistry [1, 2], including bonding theory, coordination chemistry and geometry. RR spectra have been extensively applied to natural porphyrin-dependent systems, especially those involved in oxygen use and transport, and also to synthetic models of such biological systems [3]. A large body of data has been published, and the reader is referred to the reviews by Kitagawa and Ozaki [1] and Felton and Yu [2] for explanations of the theory and assignments of porphyrin vibrational spectra. The

commonly-used model compound *meso*-tetraphenylporphyrin ( $\text{H}_2\text{TPP}$ ) and many of its transition metal complexes have been subjected to RR analysis. Correlations with such data as spin state, electron configuration and particularly porphyrin 'core size' have been developed [4–7]. The only study of tin(IV) TPP complexes is that of Huong and Pommier [4] who reported RR spectra of one complex,  $\text{Sn}(\text{TPP})\text{Cl}_2$ , in the solid state and in dichloromethane solution.

My co-workers and I have previously studied the electronic effects of axial ligands in six-coordinate tin(IV) complexes of TPP, using visible absorption and  $^1\text{H}$  NMR spectra [8–10]. Various other structural, spectroscopic and electrochemical investigations of similar tin porphyrins have been reported [11]. The availability of the FT-Raman instrument afforded the chance of probing the bonding in the metal–porphyrin plane, and the effects of axial ligands, using non-resonance Raman spectra. The series of ligands includes the four halides, and a range of oxygen-bound anions of widely differing basicity. Some of these complexes have been characterized by single crystal X-ray diffraction [12, 13]. As mentioned by Huong and Pommier [4], the tin(IV) porphyrin complexes represent an extreme case, since the metal ion is the largest which can be accommodated in the cavity of the porphyrin, and still retain planarity in the  $\text{MN}_4$  unit. As complexes of tin(IV) with porphyrins and related ligands have attracted interest lately regarding their possible medical uses [14, 15], it is important to understand their structure and chemistry. This paper reports the Raman frequencies for the series

of complexes, and compares the data within the series, and with published data for other  $M(\text{TPP})$  complexes.

## Experimental

The  $\text{Sn}(\text{TPP})\text{X}_2$  complexes were all available from previous studies [8–10, 12]. The crystalline compounds were loosely packed into glass melting point capillaries (Kimax 34505,  $1.5-1.8 \times 90$  mm), with no grinding or other treatment. The capillary was positioned in the liquids sample holder supplied with the instrument. Scattering intensity was maximized using a capillary containing barium sulfate, and manual adjustment of the  $xyz$  positioning knobs. Spectra from  $3000-150$   $\text{cm}^{-1}$  of Raman shift were obtained with a Perkin-Elmer model 1700 FT-IR spectrometer with Raman attachment. The interferometer was fitted with a wide range germanium on KBr beamsplitter. The source was a Spectron Laser Systems SL101 Nd/YAG laser operating at 1064 nm. The detector was InGaAs, cooled to 77 K with liquid nitrogen. Laser power was 10–20 mW, chosen to give a spectrum with a convenient background intensity. Laser power in excess of about 30 mW generally caused severe degradation of the sample. Apodization was strong Beer-Norton, the default apodization function of the Perkin-Elmer spectrometer. Spectra were recorded in single beam mode at a resolution of  $2$   $\text{cm}^{-1}$ , giving a scan time of 8 s. Approximately 3000 scans gave spectra of low noise and excellent quality. Spectra were processed, displayed, manipulated and plotted using Perkin-Elmer IRDM software.

## Results and discussion

### Band assignments

Figure 1 shows the molecular structure of the complexes  $\text{Sn}(\text{TPP})\text{X}_2$ , together with conventional atom labelling. The frequencies of the Raman bands for all

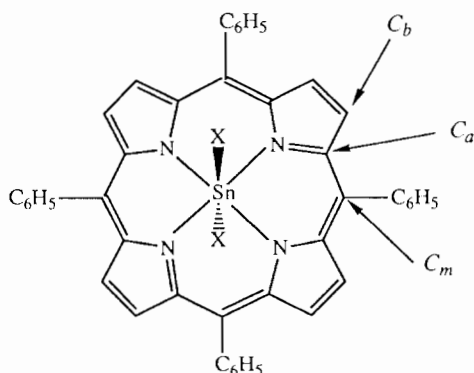


Fig. 1. General structure of the  $\text{Sn}(\text{TPP})\text{X}_2$  complexes, with atom labelling.

complexes and the free ligand  $\text{H}_2\text{TPP}$  are shown in Table 1, together with likely band assignments (see below). Weak bands which are not common to all complexes and are presumably internal axial ligand vibrations have not been included. The bands or spectral regions have been given the labels 1–17. These numbers are for convenience of reference only, and have no theoretical significance. Various systems of band numbering have been applied to RR spectra and so are not necessarily applicable here. The labelled bands are the most intense, or in some cases, the most informative or distinctive weaker bands. The region labelled 16 consists variously of from one to five components, even for monoatomic ligands, and all frequencies have been included. The spectra from  $1700$  to  $200$   $\text{cm}^{-1}$  of the free ligand and two complexes,  $\text{Sn}(\text{TPP})(\text{CF}_3\text{SO}_3)_2$  and  $\text{Sn}(\text{TPP})(\text{OH})_2$  (representing the extremes of the range of ligand basicity) are shown in Fig. 2. Data have been normalized to give spectra of comparable maximum intensities. Intensities have not been given in Table 1, as they are similar in all spectra, and a qualitative picture may be obtained from Fig. 2. Moreover, the spectra are uncorrected for either instrument or sample background, and no absolute intensity measurements have been made. Bands/regions have been labelled on Fig. 2 to correspond with Table 1. Bands 8a and 15a are found only in  $\text{H}_2\text{TPP}$ . The former is assigned with certainty to  $\delta(\text{NH})$ , while the latter has previously been tentatively assigned to a radial mode of the N–H pyrrole rings [16].

While an attempt has been made in Table 1 to assign all the significant bands, there are several factors which make some of these somewhat doubtful. Firstly, these spectra were recorded for solid samples, while literature spectra for other complexes have been recorded in various solvents, such as  $\text{CS}_2$ ,  $\text{CH}_2\text{Cl}_2$  and benzene. Secondly, various laser excitation frequencies have been used for RR spectra, and so comparison with non-resonant spectra is difficult. According to conventional theory, e.g. ref. 1, of the in-plane modes of a  $D_{4h}$  metalloporphyrin, the  $\text{A}_{2g}$  bands should be seen only in resonance enhanced spectra. Stein *et al.* [16] reported the RR spectrum of the free ligand  $\text{H}_2\text{TPP}$ , so a comparison can be made with this spectrum. Most bands are common to the two spectra, especially in the important region above  $1000$   $\text{cm}^{-1}$ . Bands at  $1492$  and  $1458$   $\text{cm}^{-1}$  in Table 1 were absent in the RR spectrum, while the RR bands at  $1357$  and  $1135$   $\text{cm}^{-1}$  are extremely weak or absent in my spectrum. Although  $\text{H}_2\text{TPP}$  is of  $D_{2h}$  symmetry in the solid state, the similarity of these spectra encourages confidence that comparisons of the RR and non-resonance spectra will be valid. The solid state RR spectrum of  $\text{Sn}(\text{TPP})\text{Cl}_2$  reported by Huang and Pommier [4] shows close agreement with my spectrum in most band frequencies (see Table 1).

TABLE 1. Raman band frequencies ( $\text{cm}^{-1}$ ) for the free base  $\text{H}_2\text{TPP}$  and the complexes  $\text{Sn}(\text{TPP})\text{X}_2$ , with band numbering and assignments

Band no.	$\text{H}_2\text{TPP}$	$\text{CF}_3\text{SO}_3$	$\text{NO}_3$	$\text{CF}_3\text{CO}_2$	sal	$\text{HCO}_2$	$\text{PhCO}_2$	$\text{CH}_3\text{CO}_2$	OH	I	Br	Cl	Cl [4]	F	Assignment
1	1596	1599	1598	1599	1596	1599	1596	1597	1597	1598	1597	1596	1596	1595	phenyl
2	1550	1541	1537	1537	1539	1536	1538	1537	1533	1532	1534	1536	1534	1538	$\nu(\text{C}_b\text{C}_b)\text{A}_{1g}$
3	1500	1496	1496	1495	1494	1494	1493	1496	1495	1494	1494	1493		1492	phenyl
4	1492	1490	1486	1485	1485	1485	1485	1485	1480	1483	1483	1483	1485	1485	$\nu(\text{C}_b\text{C}_b)\text{B}_{1g}$
5	1458	1467	1462	1461	1459	1457	1458	1459	1448	1455	1456	1454	1460	1455	$\nu(\text{C}_a\text{C}_b)\text{A}_{1g}$
6	1440	1439	1437	1440	1440	1438	1439	1439	1433	1439	1440	1438	1436	1440	$\nu(\text{C}_a\text{C}_m)\text{B}_{1g}$
											1433	1434			
7	1383	1372 <sup>a</sup>	1368 <sup>a</sup>	1370	1369 <sup>a</sup>	1369	1369	1368	1364	1366	1367	1367		1367	$\nu(\text{C}_a\text{N})\text{A}_{1g}$
8	1376	1372 <sup>a</sup>	1368 <sup>a</sup>	1364	1369 <sup>a</sup>	1363	1365	1361	1355	1358	1360	1360	1360	1363	$\nu(\text{C}_a\text{C}_b)\text{B}_{2g}$
													1353		
8a	1328 <sup>b</sup>														
9	1294	1294	1299	1300	1305	1305	1307	1303	1314	1299	1302	1308		1310	?
10		1244		1244	1236	1236	1237	1237	1240			1245		1243	phenyl, $\nu(\text{C}_a\text{N})$
		1232	1236	1234	1237		1232			1234	1234	1235	1232	1236	$\text{B}_{1g}$ , $\nu(\text{C}_m\text{Ph})\text{A}_{1g}$
11	1080	1091	1088	1090		1089	1085	1085	1084	1086	1086	1078	1083	1081	$\delta(\text{C}_b\text{H})$
12	1034	1041	1040	1040	1037	1038	1037	1039	1034	1037	1036	1035	1036	1038	phenyl, $\delta(\text{C}_b\text{H})$
							1025			1023	1024	1024	1026		
13	1002	1000	1002	1002	1000	1003	1003	1000	999	1002	1002	1002	1000	1003	phenyl, $\nu(\text{C}_a\text{C}_m)$
												992	996	$\text{A}_{1g}$	
14	664	671	662	661	662	662	661	661	663	662	663	660		663	phenyl, porph. def., $\nu(\text{SnN})?$
													634		
15	408	413	417	409	418	411	409	411	405	406	411	411	405	406	porph. def., $\nu(\text{SnN})?$
		403	405	401	408	407			396						
15a	336 <sup>c</sup>														
	329														
16		263	264	261	261	257	267	265	255	264	264		255	257	
		258	252	242	243		257	252		254	257				
			247	238			250			247					
			241			243				240					
										231					
17	212	204	205	204	201	202	202		201	201	202	200	200	203	
	202														

<sup>a</sup>Assignments may be reversed, two bands not resolved, but assumed to be present. <sup>b</sup> $\delta(\text{NH})$ . <sup>c</sup>Radial mode of pyrrole rings.

There are, as expected, several bands whose intensities differ. Bands more intense in the resonant spectrum are 10, 12 (2 bands in RR) and 15, while band 9 is absent, and band 13 is very weak in the RR spectrum. The assignment of band 2 as an  $\text{A}_{2g}$  band is not consistent with its being the most intense band in these non-resonance spectra.

The assignments given in Table 1 are derived from those of Stein *et al.* [16], Blom *et al.* [17] and Burke *et al.* [18], by considering that bands with very small axial ligand shifts are probably largely phenyl vibrations, and that  $\text{A}_{2g}$  bands will be absent or very weak. In general, one expects the stretching frequency order to be  $\text{C}_b\text{C}_b > \text{C}_a\text{C}_m \cong \text{C}_a\text{N} > \text{C}_a\text{C}_b > \text{C}_m\text{C}_{\text{Ph}}$  [18], but such an

order is never clear-cut since all vibrations have contributions from more than one mode. By considering the axial ligand shifts (see below), a reasonably self consistent set of assignments arises, which has only some anomalous features. Firstly, there is some doubt about the bands labelled 3 and 4. Band 3, near  $1495 \text{ cm}^{-1}$ , changes very little with the axial ligand, so may be a phenyl associated mode. Such a band has not been reported in RR spectra of  $\text{M}(\text{TPP})$  complexes. However, in the Raman spectrum of biphenyl, an  $\text{A}_{1g}$  band is observed at  $1507 \text{ cm}^{-1}$  [19]. Band 4, which varies from  $1490$  ( $\text{X} = \text{CF}_3\text{SO}_3$ ) to  $1480$  ( $\text{X} = \text{OH}$ )  $\text{cm}^{-1}$ , seems to correspond to the  $\nu(\text{C}_b\text{C}_b)(\text{B}_{1g})$  mode reported for many  $\text{M}(\text{TPP})$  derivatives, e.g.  $1505 \text{ cm}^{-1}$  for

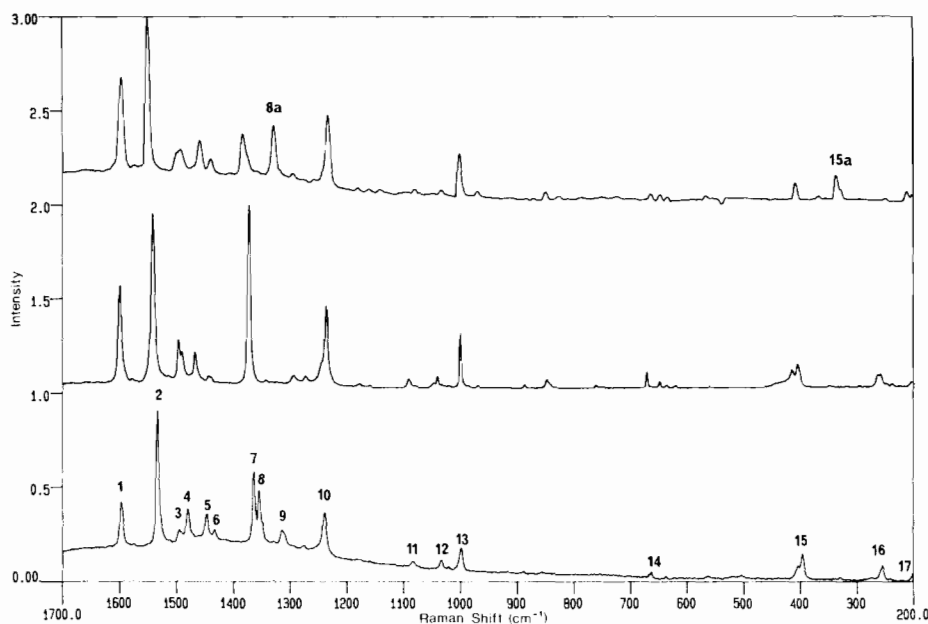


Fig. 2. Representative FT-Raman spectra: top,  $\text{H}_2\text{TPP}$ ; middle,  $\text{Sn}(\text{TPP})(\text{CF}_3\text{SO}_3)_2$ ; bottom,  $\text{Sn}(\text{TPP})(\text{OH})_2$ . Band numbers correspond to those in Table 1. Ordinates of the spectra have been normalized and modified for clarity of display.

$[\text{Fe}(\text{TPP})(\text{imidazole})_2]\text{Cl}$  [18]. The  $1500\text{ cm}^{-1}$  band of  $\text{H}_2\text{TPP}$  was assigned to this mode by Stein *et al.* [16]. An alternative assignment would be as follows. Band 3 may be the  $\nu(\text{C}_b\text{C}_b)(\text{B}_{1g})$  mode, and band 4 would then correspond to the  $\nu_{as}(\text{C}_a\text{C}_m)(\text{A}_{2g})$  mode (e.g.  $1540\text{ cm}^{-1}$  in  $[\text{Fe}(\text{TPP})(\text{imidazole})_2]\text{Cl}$  [18]). This is hard to support, however, because (i)  $\text{A}_{2g}$  modes should be very weak; (ii) band 2, which seems likely to be the  $\nu(\text{C}_b\text{C}_b)(\text{A}_{1g})$  mode, is axial ligand sensitive, so why should its  $\text{B}_{1g}$  mode be structure insensitive? Further clarification of this point will require deuteration or polarization experiments, which are beyond the scope of the present studies.

The second assignment problem arises with the bands labelled 7 and 8, near  $1360\text{ cm}^{-1}$ . These are presumed to be largely the  $\nu(\text{C}_a\text{N})(\text{A}_{1g})$  and  $\nu_{as}(\text{C}_a\text{C}_b)(\text{B}_{2g})$  vibrations, by analogy with various other TPP complexes, but the order of these is impossible to assign with any certainty. The weak band labelled 9 is also a problem, as no comparable band has been assigned in published work. As will be described below, this band also has an anomalous axial ligand dependence. At present, this band remains unassigned. Assignments in the region below  $1000\text{ cm}^{-1}$  are also difficult because they involve various porphyrin deformations, out-of-plane modes, and metal ligand modes.

#### Correlations within the series

There are several bands in the Raman spectra which display sensitivity to axial ligand variation. While some bands, e.g. 1, 3, 10 and 13, exhibit a variation of only  $1\text{--}2\text{ cm}^{-1}$ , bands 2, 4, 6, 7, 11 and 12 vary over a range

of  $6\text{--}10\text{ cm}^{-1}$ , and the set 5, 8 and 9 shows a range of  $17\text{--}20\text{ cm}^{-1}$ . This is a considerable change for a single metal ion and oxidation state, but earlier NMR studies have also shown that the bonding in the tin-porphyrin plane is very sensitive to the basicity of the axial ligands [8–10]. For example,  $^4J(\text{Sn-H})$ , the coupling constant between the tin nucleus and the peripheral  $\beta$ -pyrrole protons, varies from 10.4 Hz in  $\text{Sn}(\text{TPP})(\text{OH})_2$  to 20 Hz for  $\text{Sn}(\text{TPP})(\text{CF}_3\text{SO}_3)_2$  [8, 12]. The NMR and visible absorption spectral results showed that the O-bound ligands and the halides must be considered separately, since ligand basicity dominates in the former complexes, but  $\pi$ -bonding effects must be considered for the latter [8, 10].

Figures 3 and 4 are plots of the most sensitive Raman frequencies against  $\text{p}K_a$  of the axial anion. Good correlations are shown with  $\text{p}K_a$  for the O-bound ligands, and the expected trend is seen for all except band 9. A more basic axial ligand places more demand on the tin electrons and this is manifest in a weaker bonding throughout the porphyrin unit. Thus lower frequencies are seen for vibrations of  $\text{C}_a\text{--N}$ ,  $\text{C}_a\text{--C}_b$ ,  $\text{C}_b\text{--C}_b$  and  $\text{C}_a\text{--C}_m$  bonds. Such dependence on  $\text{p}K_a$  of axial ligands has been demonstrated for a series of  $\text{Fe}(\text{OEP})\text{L}_2$  complexes (OEP = octaethylporphyrin, L = 4-substituted pyridines), although the substituent effects in this system are naturally quite small, given the distance between the varying substituent and the metal, and the smaller  $\text{p}K_a$  range [20]. The halides, as expected from earlier work [8, 10], show much less variation in frequency for all bands, usually only *c.*  $1\text{--}2\text{ cm}^{-1}$  from F to I; and with no discernable pattern. Again however, the

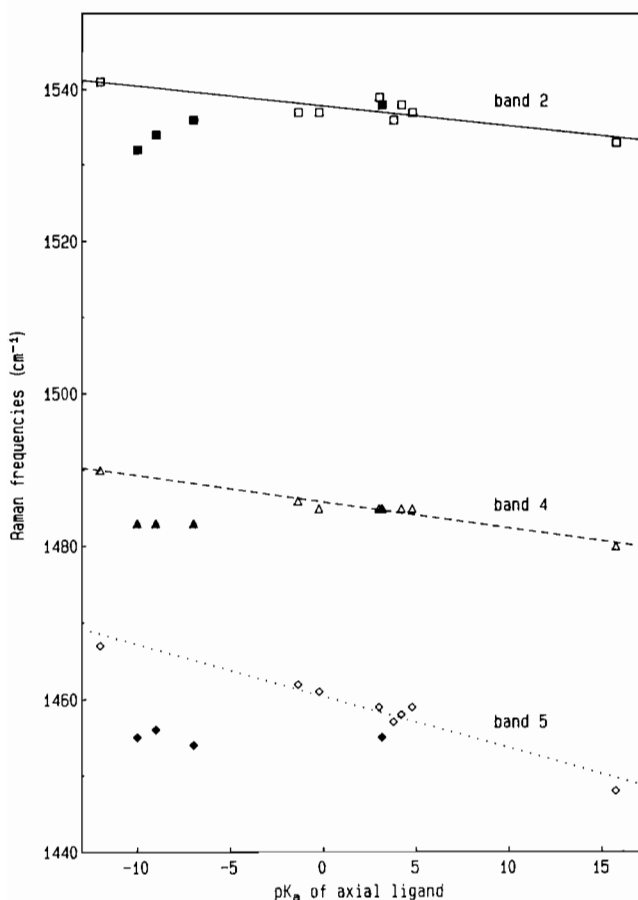


Fig. 3. Variation of the Raman shifts of bands 2, 4 and 5 with  $pK_a$  of the axial anion. Oxygen-bound ligands are shown by open symbols, halides by filled symbols. Regression lines include only the former points.

most sensitive band is band 9, whose  $pK_a$  dependence is non-linear. The trend is in the same direction as for the O-bound anions, i.e. the frequency *increases* with ligand basicity. To confuse the picture further, band 2 shows a similar anomalous non-linear dependence on halide basicity, while the O-bound anion dependence is in the usual sense. The behaviour of band 9 is so exceptional that one could suspect it to be an artefact. This is hard to sustain, since, although this band is weak, it is clearly seen in all spectra, and it displays a good correlation with  $pK_a$  ( $r=0.963$ ).

Figures 5 and 6 show plots of the same five band frequencies against another parameter expected to reflect electronic effects. This is the frequency of the longest wavelength visible absorption band, designated as the  $\alpha$  band, which is found in the region 588–614 nm for these Sn(TPP) complexes [8]. Shelnutt and Ondrias, and others [21], have previously discussed the relationship between  $\lambda_\alpha$  and various Raman band frequencies in metal octaalkylporphyrin complexes. In the Sn(TPP) series, good correlations are again found for the O-bound anions, such that a strengthening of bonds

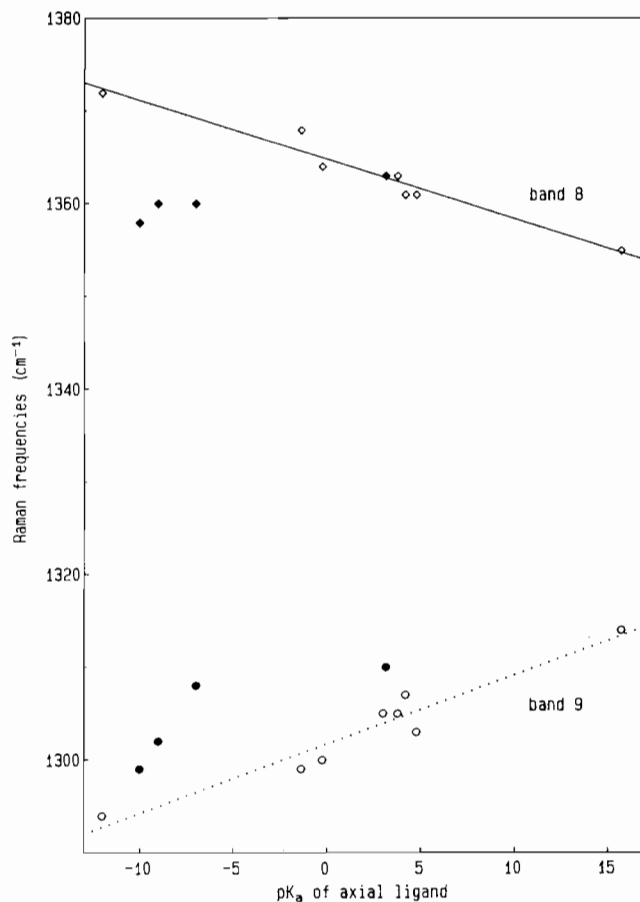


Fig. 4. Variation of the Raman shifts of bands 8 and 9 with  $pK_a$  of the axial anion. Oxygen-bound ligands are shown by open symbols, halides by filled symbols. Regression lines include only the former points.

in the porphyrin framework reflects a decrease in  $\lambda_\alpha$ , again with the exception of band 9. In the halide complexes, chemical shifts, coupling constants and Raman frequencies change very little from F to I. However, the  $\lambda_\alpha$  and absorption coefficient ratios  $\epsilon_\beta/\epsilon_\alpha$  do change markedly in this series, so these parameters appear to reflect most closely the  $\pi$ -acceptance properties of the axial ligand. It should be noted that band 9 shows 'normal' behaviour for the halides, i.e. bond strengthening follows the  $\pi$ -acceptance tendency. The relationship of bond lengths to Raman frequencies is discussed in the next section.

#### Correlations with other TPP complexes

Resonance Raman spectra of M(TPP) complexes have previously been related to crystallographically determined bond lengths [4–7, 22, 23]. The parameter 'core size' is a measure of the size of the cavity in the porphyrin ligand in a complex. This parameter, denoted  $r(\text{Ct-N})$ , is the average distance from the four nitrogen atoms to the point where the projection of the metal ion meets the average plane of the four nitrogens. This

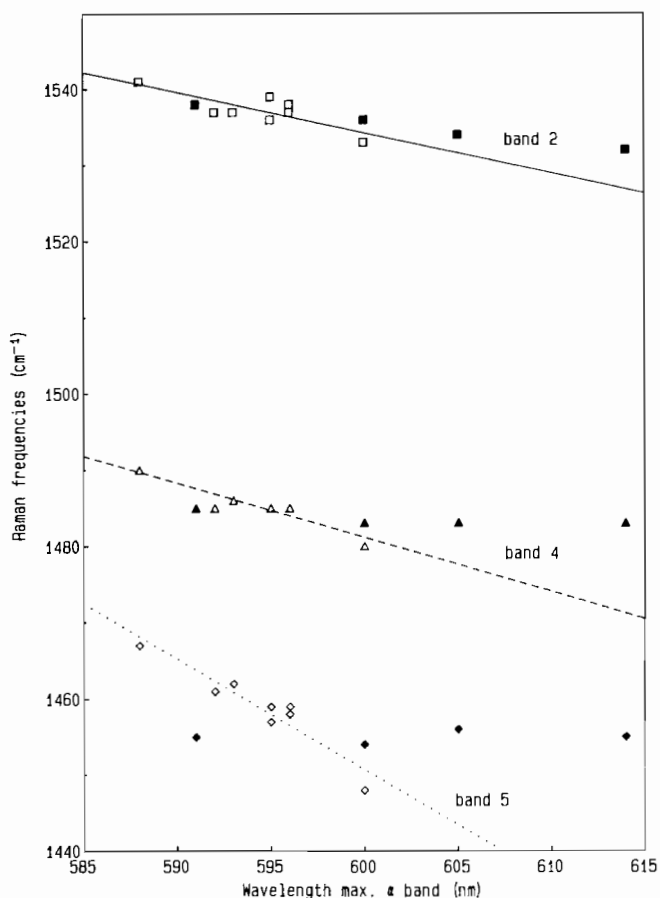


Fig. 5. Relationship between Raman shifts of bands 2, 4 and 5 and the wavelength maximum of the  $\alpha$  visible absorption band. Oxygen-bound ligands are shown by open symbols, halides by filled symbols. Regression lines include only the former points.

quantity allows comparison between four-, five- and six-coordinate complexes, and the various metalloporphyrin geometries, planar ( $D_{4h}$ ), ruffled ( $S_4$ ) or domed ( $C_{2v}$  or  $C_{4v}$ ). Various empirical correlations have been proposed which relate Raman frequencies with  $r(\text{Ct-N})$ . Huang and Pommier [4], Stong *et al.* [6] and Chottard *et al.* [7] calculated linear equations for various bands, using different data sets. Given the large variations in Raman frequencies across the series of  $\text{Sn}(\text{TPP})\text{X}_2$  complexes, correlations across various porphyrins, metals, axial ligands and coordination types should not be expected to be valid except as rather vague predictors of trends. The published correlations display considerable scatter, perhaps not surprisingly, as many are based on solution Raman spectra. The predictive value of one equation was very poor for the series  $\text{Ni}(\text{TPP})\text{-Pt}(\text{TPP})$  [22, 24]. Even when a suitably restricted data set is used, e.g. a series of six-coordinate  $\text{M}(\text{TPP})$  complexes, fair correlations are found with some bands, but effects such as spin state in Fe complexes can override apparent geometrical effects. Application of some of the proposed equations to the tin(IV)

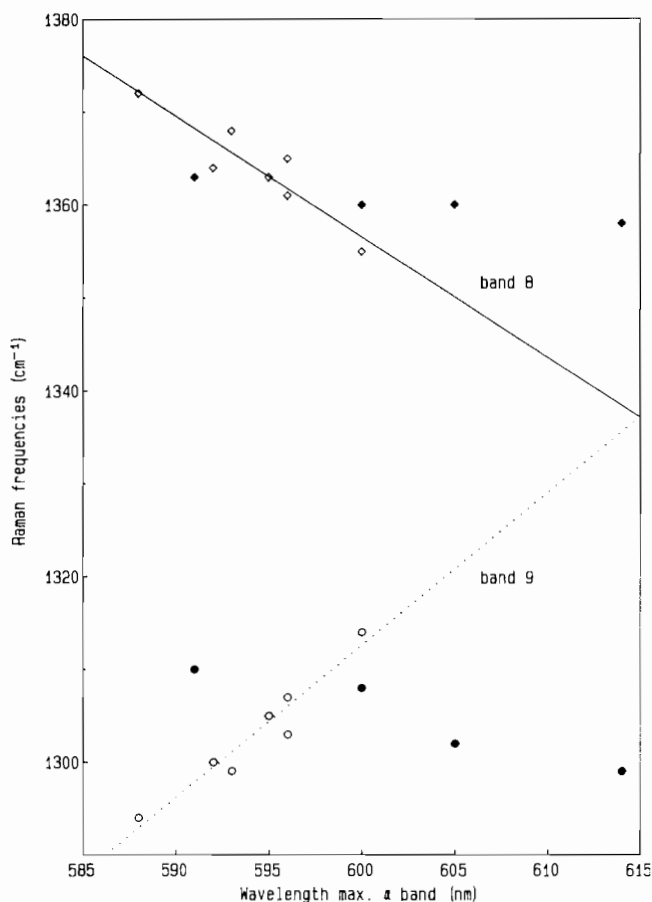


Fig. 6. Relationship between Raman shifts of bands 8 and 9 and the wavelength maximum of the  $\alpha$  visible absorption band. Oxygen-bound ligands are shown by open symbols, halides by filled symbols. Regression lines include only the former points.

complexes is worthwhile since, as stated earlier, the tin complexes represent the extreme in core size expansion for complexes with approximate  $D_{4h}$  symmetry. The Huang and Pommier [4] equation applies to ' $\nu_a$ ', originally assigned as the  $\nu(\text{C}_b\text{-C}_b)(A_{2g})$  mode,  $r(\text{Ct-N}) = 4.860 - 0.0018 \nu_a$ . The solid state structures of  $\text{Sn}(\text{TPP})(\text{OH})_2$  [12] and  $\text{Sn}(\text{TPP})\text{Cl}_2$  [13] are known to high precision, and they both have imposed exact  $D_{4h}$  symmetry. The Sn-N distances are 2.106(3) and 2.098(2) Å, respectively. The structures of  $\text{Sn}(\text{TPP})(\text{benzoate})_2$ ,  $\text{Sn}(\text{TPP})(\text{salicylate})_2$  and  $[\text{Sn}(\text{TPP})(\text{H}_2\text{O})_2](\text{CF}_3\text{SO}_3)_2$  are known to lower precision, but clearly their average M-N distances are slightly shorter at 2.087(5), 2.09(1) and 2.06(2) Å [12]. The diaquo complex is expected to resemble the covalent form  $\text{Sn}(\text{TPP})(\text{CF}_3\text{SO}_3)_2$  in its bond lengths.

The equation of Huang and Pommier [4] predicts less change than that which is observed (e.g. for the trifluoromethanesulfonate, the M-N distance is calculated to be *c.* 2.086 Å). The correlation equations generated by Stong *et al.* [6], which are based on a variety of ligands, and apparently on some erroneous

points (see Table 2 in ref. 6), actually predict the frequencies of two bands in  $\text{Sn}(\text{TPP})\text{Cl}_2$  and  $\text{Sn}(\text{TPP})(\text{OH})_2$  rather well. The respective observed (calc.) values for these two complexes are 1536 (1536) and 1533 (1534)  $\text{cm}^{-1}$  for one band, and 1483 (1485) and 1480 (1481)  $\text{cm}^{-1}$  for the other. Used in the reverse sense, these correlations suggest an M–N distance of 2.080 Å (high frequency band) and 2.089 Å (low frequency band) for the trifluoromethanesulfonate complex, again probably overestimating this distance. The third band plotted by Stong *et al.* [6] is predicted at c. 1410  $\text{cm}^{-1}$  for  $\text{Sn}(\text{TPP})(\text{OH})_2$  using its Sn–N bond length, but no such band is observed. Instead, the band assigned to this vibration,  $\nu(\text{C}_a\text{C}_b)(\text{A}_{1g})$ , appears in the region 1448–1467  $\text{cm}^{-1}$  for the tin complexes. The nearest other band is in the range 1433–1439  $\text{cm}^{-1}$ . This illustrates the difficulty of finding broadly applicable relationships and certainly casts doubt on their validity when different porphyrin ligands are being compared.

This study has demonstrated the application of the near-IR FT-Raman technique to fluorescent metalloporphyrins, and has allowed comparison of Raman data with previous spectroscopic and structural studies of this series of closely related complexes. The anomalous behaviour of band 9 warrants further investigation, perhaps using deuterated TPP, other porphyrin ligands and other metals, and this will be pursued in the future.

### Acknowledgements

Q.U.T. is indebted to Perkin-Elmer for the loan of the Raman instrument. I thank Dr P. Fredericks for assistance with the instrument and software, Mr C. deBakker for recording many of the spectra, Ms E. Morrison for preparing some samples, and Q.U.T. for financial assistance.

### References

- 1 T. Kitagawa and Y. Ozaki, in J. W. Buchler (ed.), *Metal Complexes with Tetrapyrrole Ligands I*, Springer, Berlin, 1987, p. 71.
- 2 R. H. Felton and N.-T. Yu, in D. Dolphin (ed.), *The Porphyrins*, Vol. 3, Academic Press, New York, 1978, p. 347.
- 3 T. G. Spiro, in A. B. P. Lever and H. B. Gray (eds.), *Iron Porphyrins*, Vol. 2, Addison-Wesley, Reading, MA, 1983, p. 91.
- 4 P. V. Huong and J.-C. Pommier, *C.R. Acad. Sci., Ser. C*, 285 (1977) 519.
- 5 J. M. Burke, J. R. Kincaid, S. Peters, R. R. Gagne, J. P. Collmann and T. G. Spiro, *J. Am. Chem. Soc.*, 100 (1978) 6083.
- 6 J. D. Stong, T. G. Spiro, R. J. Kubaska and S. I. Shupack, *J. Raman Spectrosc.*, 9 (1980) 312.
- 7 G. Chottard, P. Battioni, J.-P. Battioni, M. Lange and D. Mansuy, *Inorg. Chem.*, 20 (1981) 1718.
- 8 D. P. Arnold, *Polyhedron*, 5 (1986) 1957.
- 9 D. P. Arnold, *Polyhedron*, 7 (1988) 225.
- 10 D. P. Arnold, E. A. Morrison and J. V. Hanna, *Polyhedron*, 9 (1990) 1331.
- 11 R. Guillard, C. Ratti, J.-M. Barbe, D. Dubois and K. M. Kadish, *Inorg. Chem.*, 30 (1991) 1537, and refs. therein.
- 12 G. Smith, D. P. Arnold, C. H. L. Kennard and T. W. Mak, *Polyhedron*, 10 (1991) 509.
- 13 D. M. Collins, W. R. Scheidt and J. L. Hoard, *J. Am. Chem. Soc.*, 94 (1972) 6689.
- 14 G. S. Drummond, R. A. Galbraith, M. K. Sardana and A. Kappas, *Arch. Biochem. Biophys.*, 255 (1987) 64.
- 15 A. R. Morgan, G. M. Garbo, R. W. Keck and S. H. Selman, *Cancer Res.*, 48 (1988) 194.
- 16 P. Stein, A. Ulman and T. G. Spiro, *J. Phys. Chem.*, 88 (1984) 369.
- 17 N. Blom, J. Odo, K. Nakamoto and D. P. Strommen, *J. Phys. Chem.*, 90 (1986) 2847.
- 18 J. M. Burke, J. R. Kincaid and T. G. Spiro, *J. Am. Chem. Soc.*, 100 (1978) 6077.
- 19 G. Zerbi and S. Sandroni, *Spectrochim. Acta, Part A*, 24 (1968) 483.
- 20 Y. Ozaki, K. Iriyama, H. Ogoshi, T. Ochai and T. Kitagawa, *J. Phys. Chem.*, 90 (1986) 6105.
- 21 J. A. Shelnutz and M. R. Ondrias, *Inorg. Chem.*, 23 (1984) 1175, and refs. therein.
- 22 J.-C. Seo, Y.-B. Chung and D. Kim, *Appl. Spectrosc.*, 41 (1987) 1199.
- 23 H. Oshio, T. Ama, T. Watanabe, J. Kincaid and K. Nakamoto, *Spectrochim. Acta, Part A*, 40 (1984) 863.
- 24 A. Hazell, *Acta Crystallogr., Sect. C*, 40 (1984) 751.